World Journal of Radiology

Submit a Manuscript: http://www.wjgnet.com/esps/
Help Desk: http://www.wjgnet.com/esps/helpdesk.aspx
DOI: 10.4329/wjr.v6.i5.192

World J Radiol 2014 May 28; 6(5): 192-202
ISSN 1949-8470 (online)

ORIGINAL ARTICLE

Atherosclerosis imaging using 3D black blood TSE SPACE *vs* 2D TSE

Stephanie K Wong, Motunrayo Mobolaji-Iawal, Leron Arama, Joy Cambe, Sylvia Biso, Nadia Alie, Zahi A Fayad, Venkatesh Mani

Stephanie K Wong, Motunrayo Mobolaji-Iawal, Leron Arama, Joy Cambe, Sylvia Biso, Nadia Alie, Zahi A Fayad, Venkatesh Mani, Translational and Molecular Imaging Institute, Icahn School of Medicine at Mt. Sinai, New York, NY 10029, United States

Stephanie K Wong, Motunrayo Mobolaji-Iawal, Zahi A Fayad, Venkatesh Mani, Department of Radiology, Icahn School of Medicine at Mt. Sinai, New York, NY 10029, United States

Zahi A Fayad, Zena and Michael A Wiener Cardiovascular Institute, Department of Medicine, Marie-Josée and Henry R, Kravis Cardiovascular Health Center, Icahn School of Medicine at Mt. Sinai, New York, NY 10029, United States

Author contributions: Wong SK made substantial contributions to data analysis and interpretation, performed the statistical analysis, wrote the manuscript draft, and revised it critically according the suggestions of the other authors; Mobolaji-Iawal M, Cambe J, Biso S and Alie N made substantial contributions to data analysis, interpretation, finding the pictures, and helped draft the manuscript; Arama L participated in the design of the study and made substantial contribution to data analysis; Fayad ZA made substantial contribution to study conception and design, and critically revised the manuscript draft for important intellectual content; Mani V made substantial contributions to the study conception and design, participated in data acquisition, critically revised the manuscript draft for important intellectual content, and gave final approval of the version to be published; all the authors read and approved the final manuscript.

Supported by NIH NHLBI R01HL71021 (Fayad ZA); and Siemens Medical Solutions

Correspondence to: Venkatesh Mani, PhD, Assistant Professor, Translational and Molecular Imaging Institute, Icahn School of Medicine at Mt. Sinai, One Gustave L, Levy Place, Box 1234, New York, NY 10029, United States. venkatesh.mani@mssm.edu
Telephone: +1-212-8248454 Fax: +1-646-5379689

Received: December 21, 2013 Revised: January 30, 2014
Accepted: April 17, 2014
Published online: May 28, 2014

Abstract

AIM: To compare 3D Black Blood turbo spin echo (TSE) sampling perfection with application-optimized contrast using different flip angle evolution (SPACE) *vs* 2D TSE in evaluating atherosclerotic plaques in multiple vascular territories.

METHODS: The carotid, aortic, and femoral arterial walls of 16 patients at risk for cardiovascular or atherosclerotic disease were studied using both 3D black blood magnetic resonance imaging SPACE and conventional 2D multi-contrast TSE sequences using a consolidated imaging approach in the same imaging session. Qualitative and quantitative analyses were performed on the images. Agreement of morphometric measurements between the two imaging sequences was assessed using a two-sample *t*-test, calculation of the intra-class correlation coefficient and by the method of linear regression and Bland-Altman analyses.

RESULTS: No statistically significant qualitative differences were found between the 3D SPACE and 2D TSE techniques for images of the carotids and aorta. For images of the femoral arteries, however, there were statistically significant differences in all four qualitative scores between the two techniques. Using the current approach, 3D SPACE is suboptimal for femoral imaging. However, this may be due to coils not being optimized for femoral imaging. Quantitatively, in our study, higher mean total vessel area measurements for the 3D SPACE technique across all three vascular beds were observed. No significant differences in lumen area for both the right and left carotids were observed between the two techniques. Overall, a significant-correlation existed between measures obtained between the two approaches.

CONCLUSION: Qualitative and quantitative measurements between 3D SPACE and 2D TSE techniques are comparable. 3D-SPACE may be a feasible approach in the evaluation of cardiovascular patients.

Key words: Atherosclerosis; Carotid artery plaque; Aorta; Femoral artery; Magnetic resonance imaging

Core tip: The traditional approach to atherosclerotic plaque imaging using magnetic resonance (MR) is the two-dimensional (2D) multi-contrast turbo spin echo technique. However, 3D black blood MR imaging is becoming the preferred methodology for evaluating plaque burden non-invasively. Comparing imaging results obtained using both 3D sampling Perfection with application-optimized contrast using different flip angle evolution (SPACE) and conventional 2D multi-contrast TSE sequences in evaluating vascular territories showed good agreement in both qualitative and quantitative measurements between the two techniques. 3D SPACE technique is a promising and potentially feasible approach for the evaluation of multiple vascular beds in patients at risk for cardiovascular disease.

Wong SK, Mobolaji-Iawal M, Arama L, Cambe J, Biso S, Alie N, Fayad ZA, Mani V. Atherosclerosis imaging using 3D black blood TSE SPACE *vs* 2D TSE. *World J Radiol* 2014; 6(5): 192-202 Available from: URL: http://www.wjgnet.com/1949-8470/full/v6/i5/192.htm DOI: http://dx.doi.org/10.4329/wjr.v6.i5.192

INTRODUCTION

Since atherosclerosis is a systemic disease that affects all vascular beds[1,2], Magnetic resonance imaging (MRI) can be useful in monitoring its outcomes throughout the whole body. In the past decade, MRI has emerged as a versatile imaging modality for *in vivo*, non-invasive assessment of blood vessels morphology and vessel walls composition[3-6]. More specifically, MRI has been used extensively for assessment of plaque burden of multiple vascular beds including the carotids, aorta and peripheral arteries[7-9]. By virtue of its non-invasive-non-radioactive nature, and the ability to provide high resolution *in vivo* images of multiple vascular beds, MRI is a powerful and important imaging modality that has become the method of choice for many applications[10].

Three-dimensional (3D) black blood MRI is quickly becoming the preferred methodology for evaluating atherosclerotic plaque burden non-invasively[11,12]. It is an increasingly common imaging approach employed in multiple vascular beds including the carotid[13], aorta[14,15], and femoral arteries[16] in an attempt to evaluate systemic disease burden instead of focusing on specific lesions. In such instances, 3D black-blood approaches can subsequently be used as a measure to evaluate changes in burden in response to treatment and/or evaluate progression or regression of disease over time[17]. Due to a higher SNR and decreased susceptibility of volume averaging artifacts, 3D approaches are often preferred to the conventional 2D approaches. The ability to obtain isotropic voxels thereby enabling multi-planar reformatting of images is yet another benefit of 3D approaches.

The most promising 3D black blood turbo spin echo (TSE) sequence approach currently being investigated is the sampling perfection with application-optimized contrast using different flip angle evolution (SPACE) approach[18]. Before this technique can become clinically applicable, however, its robustness in multiple vascular territories must be established. The purpose of this study was to qualitatively and quantitatively compare imaging results obtained using both 3D SPACE and conventional 2D multi-contrast TSE sequences in evaluating the carotids, aorta, and superficial femoral arteries in patients at risk for cardiovascular disease using a consolidated imaging approach in the same imaging session.

MATERIALS AND METHODS

Study population

Carotid, aortic, and femoral arterial wall imaging using both 3D SPACE and conventional 2D TSE sequences were performed on 16 patients at risk for cardiovascular or atherosclerotic disease. Patient's age, gender, family history, smoking status, lipid profile, hypertension, and diabetes were examined for inclusion in this study. To be included as a patient in the study, an individual had to have at least two or more risk factors for atherosclerosis. Informed consent was obtained from all subjects in accordance with the institutional review board at Mount Sinai School of Medicine before the imaging procedures were performed.

MR imaging

All MR images were obtained on a 1.5 T Siemens whole body MRI system (Siemens Avanto)[19]. Imaging was divided into 3 segments for appropriate anatomical coverage. In the first segment, the bilateral carotid artery extending 3 cm below and above the carotid bifurcations were imaged using a 4-channel carotid coil. In the second segment, the entire length of the aorta from the aortic arch to the iliac bifurcation was imaged using the spine array and two body matrix coils. In the last segment, the iliacs and the bilateral superficial femoral artery were imaged using the same spine array and a third body matrix coil. The patient was not repositioned on the table between the imaging of the different segments and all imaging was completed in a single session.

Imaging protocol

A 3D non-cardiac and respiratory gated SPACE sequence was utilized for the acquisition of bilateral carotid and femoral arterial images, while a 3D cardiac gated scan with navigator control for respiratory gating SPACE sequence was acquired for aortic images. Image resolution referred by the isotropic voxel size was approximately 0.78 mm^3 for the carotids, 1.1 mm^3 for the aorta, and 1.0 mm^3 for the bilateral femoral arteries. For comparison purposes, 12 slice 2D TSE images using multi-contrast weightings and parallel saturations bands for flow suppression (FS) were also obtained for the

Table 1 Imaging parameters

	2D	3D SPACE
Carotids	Axial	Coronal
FOV	140	200
TR	2000	1600
TE	56	128
Aorta	Axial	Double oblique
FOV	300	300
TR	2000	1600
TE	48	128

FOV: Field of view; TR: Repetition time; TE: Echo time; 3D: Three-dimensional.

three different vascular beds[20,21]. The in-plane resolution for 2D scans was 0.7 mm^2 for aorta, and 0.5 mm^2 for both bilateral carotid and femoral arteries. Slice thickness was 3 mm in carotids, 5 mm in aorta and 4 mm in the femoral arteries. Registration between 3D and 2D TSE images and reformatting of 3D images into axial images with a slick thickness of 3.0 mm and slice gap of 1.5 mm were performed on an MRI workstation (Leonardo; Siemens Medical Solutions, Erlangen, Germany). Total imaging time for the 3D scans was < 45 min for all three vascular beds combined. The 2D scans took 45 min to cover the same vascular territory. More detailed imaging parameters are found in Table 1. Images using 2D TSE and 3D SPACE were successfully acquired from all 16 subjects for the three vascular beds including the aorta, carotids, and femoral arteries. The order of the 3D and 2D imaging sequences was randomized for all three territories to avoid any bias.

Statistical analysis

MR images were qualitatively analyzed by an experienced reader (VM) based on 4 distinct criteria [overall image clarity, vessel wall delineation (VWD), FS, and artifacts] using a 5-point scale ranging from 1-5 with 1 being poor and 5 being excellent[22,23]. A Mann-Whitney rank sum test was used to compare the scores obtained from the qualitative analysis. A *P*-value of < 0.05 was considered significant. In addition, a morphometric, quantitative analysis using a FDA-approved, customized software program (QPlaque MR, Medis medical imaging systems, The Netherlands) was performed on all images of all subjects from both 3D and 2D TSE sequences. A trained reader analyzed the images of all 16 subjects. Outer wall area (OWA), wall thickness (WT), lumen area (LA), and total vessel area (TVA) were automatically calculated by the software based on the manually-drawn contours[24-26]. Agreement of morphometric measurements between the two imaging sequences was assessed using a two-sample *t*-test, calculation of the intraclass correlation coefficient (IBM SPSS Statistics Standard, SPSS) and by the method of linear regression and Bland-Altman analyses. For all tests, a $P < 0.05$ was considered statistically significant.

RESULTS

For this study, 16 patients were studied. Since quantitative analyses were performed on matched observations, only at most 15 pairs of patients' data were included in each respective quantitative analysis [right common carotid (RCC); left common carotid (LCC); right femoral (RF); left femoral (LF); $N_{Aorta} = 15$, $N_{RCC} = 13$, $N_{LCC} = 15$, $N_{RF} = 8$, $N_{LF} = 11$]. Sample MR images obtained from the three vascular beds using both 3D SPACE and 2D TSE sequences are shown in Figure 1.

Table 2 Mean and standard deviation of qualitative assessments

Vessel	Sequence	ImQ	VWD	FS	Artifacts
Carotids	2D TSE	4.0 ± 0.67	4.3 ± 0.67	4.2 ± 0.63	4.1 ± 0.73
Carotids	SPACE	3.7 ± 0.67	4.2 ± 0.78	4.5 ± 0.52	3.9 ± 0.73
Aorta	2D TSE	3.9 ± 0.73	4.0 ± 0.67	3.8 ± 0.63	3.4 ± 0.84
Aorta	SPACE	4.0 ± 0.67	4.3 ± 0.82	4.1 ± 0.56	3.6 ± 0.84
Femoral	2D TSE	3.9 ± 0.73	3.4 ± 0.84	3.5 ± 0.85	4.0 ± 0.67
Femoral	SPACE	2.8 ± 0.79[1]	2.3 ± 0.94[1]	2.4 ± 0.96[1]	3.1 ± 0.57[1]

[1]Indicates significant difference ($P < 0.05$). Values are in mm^2. ImQ: Image quality; VWD: Vessel wall delineation; 3D: Three-dimensional; TSE: Turbo spin echo; FS: Flow suppression.

Qualitative analysis

Qualitative analysis results involving comparison of overall image quality (ImQ), VWD, FS, and artifacts scores between 3D SPACE and 2D TSE are presented in Table 2. According to the Mann-Whitney rank sum test results, no statistically significant differences in ImQ, VWD, FS, and artifacts were observed between the two techniques for carotids and aortic imaging. For femoral imaging, however, all four criteria scores from 3D SPACE sequence were significantly lower than those of images from the 2D TSE sequence ($P < 0.05$) suggesting that the 3D SPACE sequence fared more poorly in this regard.

Results of the morphometric analysis include OWA, LA, TVA, and WT measurements. The intraclass correlation coefficient and mean value ± 1 standard deviation of LA and TVA measurements are tabulated in Table 3, while the intraclass correlation coefficient and mean value ± 1 SD of the other two parameters are presented in the supplementary material (appendix).

Comparison of carotids images between 3D SPACE and 2D TSE

With respect to images of the right common carotid (RCC), significant correlation was observed for LA_{RCC} and OWA_{RCC} between the 3D SPACE and 2D TSE sequence. A trend was observed in TVA_{RCC} ($P = 0.065$) and WT_{RCC} ($P = 0.077$). According to the paired *t*-test results for RCC images, significant differences were found between 3D SPACE and 2D TSE techniques in OWA and TVA measurements. No significant mean differences, however, were observed between the two approaches in LA_{RCC} and WT_{RCC}. Scatter plots of RCC LA and RCC TVA are shown in Figure 2A and Figure 3A respectively, while that of the other RCC morphometric parameters measured are presented in the supplementary material (appendix). Bland-Altman plots of LA_{RCC} and WT_{RCC} are shown in Figure 4A and Figure 5A respectively, while

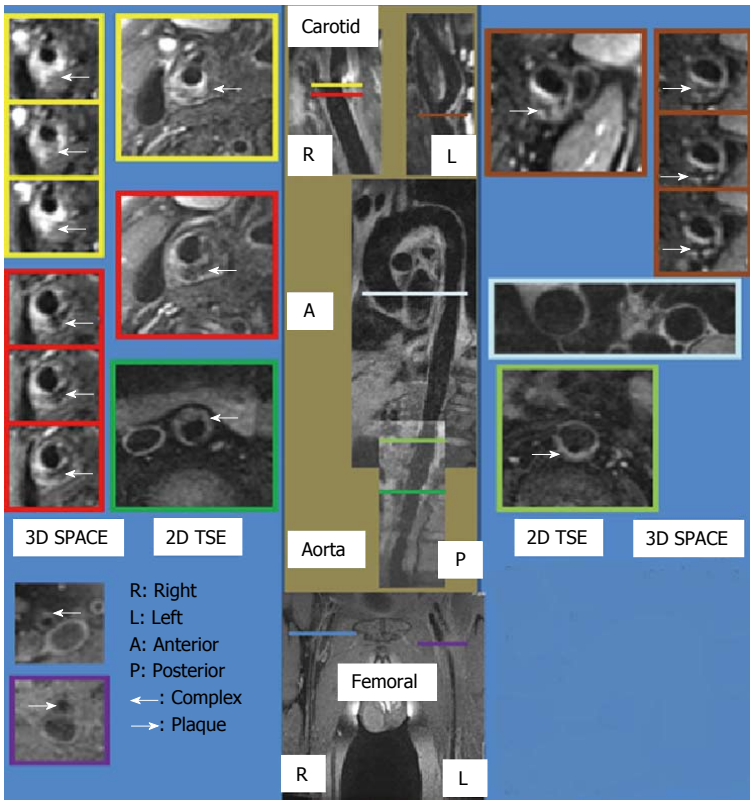

Figure 1 Sample magnetic resonance images obtained from the three vascular beds using both three-dimensional SPACE and two-dimensional turbo spin echo sequences. Montage showing samples from the two-dimensional (2D) and 3D black blood vessel wall image acquisitions of the carotids, aorta and femoral arteries acquired in a single session (longitudinal sections in the middle, cross sections on each side). Imaging time < 45 min for 3D acquisitions.

Table 3 Morphometric analysis results between three-dimensional SPACE and two-dimensional turbo spin echo images for lumen area and total vessel area

Morphometric parameter	Vessel	2D TSE	3D SPACE	[a]*P*	ICC
LA	Aorta	334.36 ± 59.42	372.74 ± 89.69[1]	0.022	0.834[1]
LA	RCC	34.76 ± 8.64	34.60 ± 11.91	0.941	0.819[1]
LA	LCC	33.58 ± 6.38	33.04 ± 9.42	0.760	0.855[1]
LA	RF	19.66 ± 9.37	20.95 ± 5.28	0.621	0.772[1]
LA	LF	27.15 ± 16.13	34.50 ± 13.95	0.066	0.818[1]
TVA	Aorta	224.29 ± 47.98	239.09 ± 63.93[1]	0.027	0.956[1]
TVA	RCC	38.19 ± 8.04	45.35 ± 11.57[1]	0.028	0.581
TVA	LCC	36.76 ± 13.32	44.35 ± 16.73[1]	0.041	0.772[1]
TVA	RF	47.42 ± 20.28	64.23 ± 15.30[1]	0.019	0.766[1]
TVA	LF	51.03 ± 17.17	71.56 ± 20.15[1]	0.001	0.808[1]

[1]Indicates statistical significant ($P < 0.05$) value. Data are mean (mm^2) of morphometric parameter value ± SD. [a]*P*: Value for mean comparison between three-dimensional (3D) SPACE and 2D turbo spin echo; LA: Lumen area; TVA: Total vessel area; RCC: Right common carotid; LCC: Left common carotid; RF: Right femoral; LF: Left femoral; ICC: Intraclass correlation coefficient.

that of the other RCC morphometric parameters measured are presented in the supplementary material (appendix). For arterial images of the LCC, there was good correlation in all four morphometric measurements from both 3D SPACE and 2D TSE sequences. According to the paired *t*-test results for LCC images, significant differences were found between 3D SPACE and 2D TSE techniques in TVA. No significant mean differences, however, were observed between the two approaches in OWA_{LCC}, LA_{LCC} and WT_{LCC}. Scatter plots of LCC LA and LCC TVA are shown in Figure 2B and Figure 3B respectively, while that of the other LCC morphometric parameters measured are presented in the supplementary material (appendix). Bland-Altman plots of LA_{LCC} and WT_{LCC} are shown in Figure 4B and Figure 5B respectively, while that of the other LCC morphometric parameters measured are presented in the supplementary material (appendix).

There was good correlation in all four aortic morphometric measurements between the 3D SPACE and 2D TSE sequences. According to the paired *t*-test results for aortic images, significant differences were found between 3D SPACE and 2D TSE techniques in OWA, LA, and TVA measurements. The difference in the mean aortic WT measurements between the two approaches, however, was not statistically significant ($P = 0.683$). Scatter plots of aortic LA and aortic TVA are shown in Figure 2C and Figure 3C respectively, while that of the other aortic morphometric parameters measured are presented in the supplementary material (appendix). Bland-Altman plots of aortic LA and aortic TVA are shown in Figure 4C and Figure 5C respectively, while that the other aortic morphometric parameters measured are presented in the supplementary material (appendix).

Comparison of femoral arteries images between 3D SPACE and 2D TSE

With respect to images of the RF artery, good correlation was observed for LA_{RF}, TVA_{RF} and WT_{RF} between the two imaging sequences, while no significant correlation was observed between the OWA_{RF} measurements ($P = 0.125$). According to the paired *t*-test results for images of the RF, significant differences were found between 3D SPACE and 2D TSE techniques in TVA

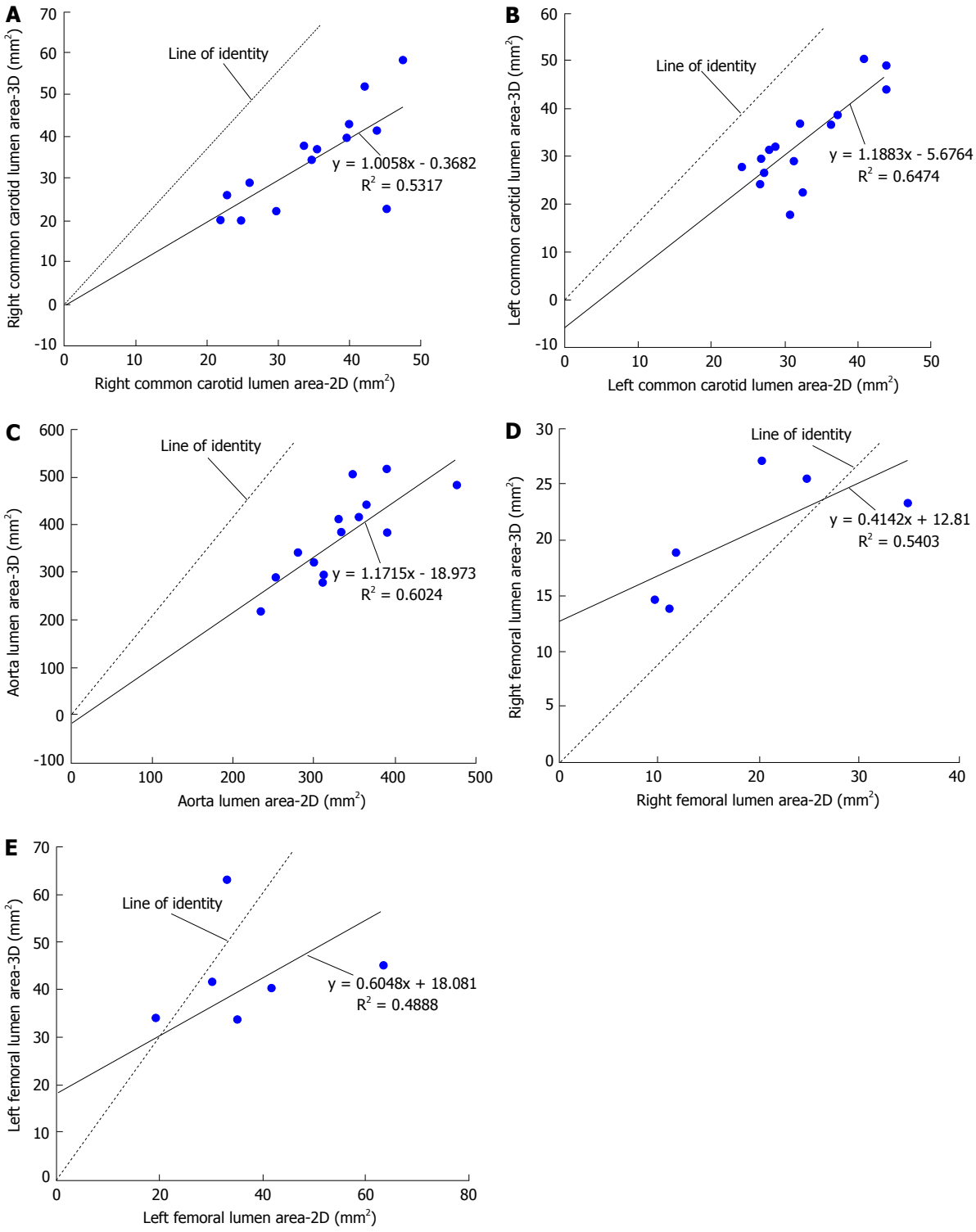

Figure 2 Scatter plots of lumen area comparing three-dimensional SPACE and two-dimensional turbo spin echo images. Morphometric analysis using a FDA-approved, customized software program (QPlaque MR, Medis medical imaging systems, The Netherlands) was performed on all carotid, aortic and femoral arterial wall images of 16 patients who were at risk for cardiovascular or atherosclerotic disease for three-dimensional (3D) SPACE and conventional 2D multi contrast turbo spin echo (TSE) sequences. A: Scatter plot of RCC lumen area comparing 3D SPACE and 2D TSE images. There was a moderate positive linear correlation (R = 0.729) between the values of the RCC lumen area obtained from the 3D SPACE and 2D TSE sequences; B: Scatter plot of LCC lumen area comparing 3D SPACE and 2D TSE images. There was a strong positive linear correlation (R = 0.805) between the values of the LCC lumen area obtained from the 3D SPACE and 2D TSE sequences; C: Scatter plot of aorta lumen area comparing 3D SPACE and 2D TSE images. There was a strong positive linear correlation (R = 0.776) between the values of the aorta lumen area obtained from the 3D SPACE and 2D TSE sequences; D: Scatter plot of RF lumen area comparing 3D SPACE and 2D TSE images. There was a moderate positive linear correlation (R = 0.735) between the values of the RF lumen area obtained from the 3D SPACE and 2D TSE sequences; E: Scatter plot of LF lumen area comparing 3D SPACE and 2D TSE images. There was a moderate positive linear correlation (R = 0.699) between the values of the LF lumen area obtained from the 3D SPACE and 2D TSE sequences. RCC: Right common carotid; LCC: Left common carotid; RF: Right femoral; LF: Left femoral.

and WT. No significant mean differences, however, were observed between the two approaches in OWA$_{RF}$, LA$_{RF}$

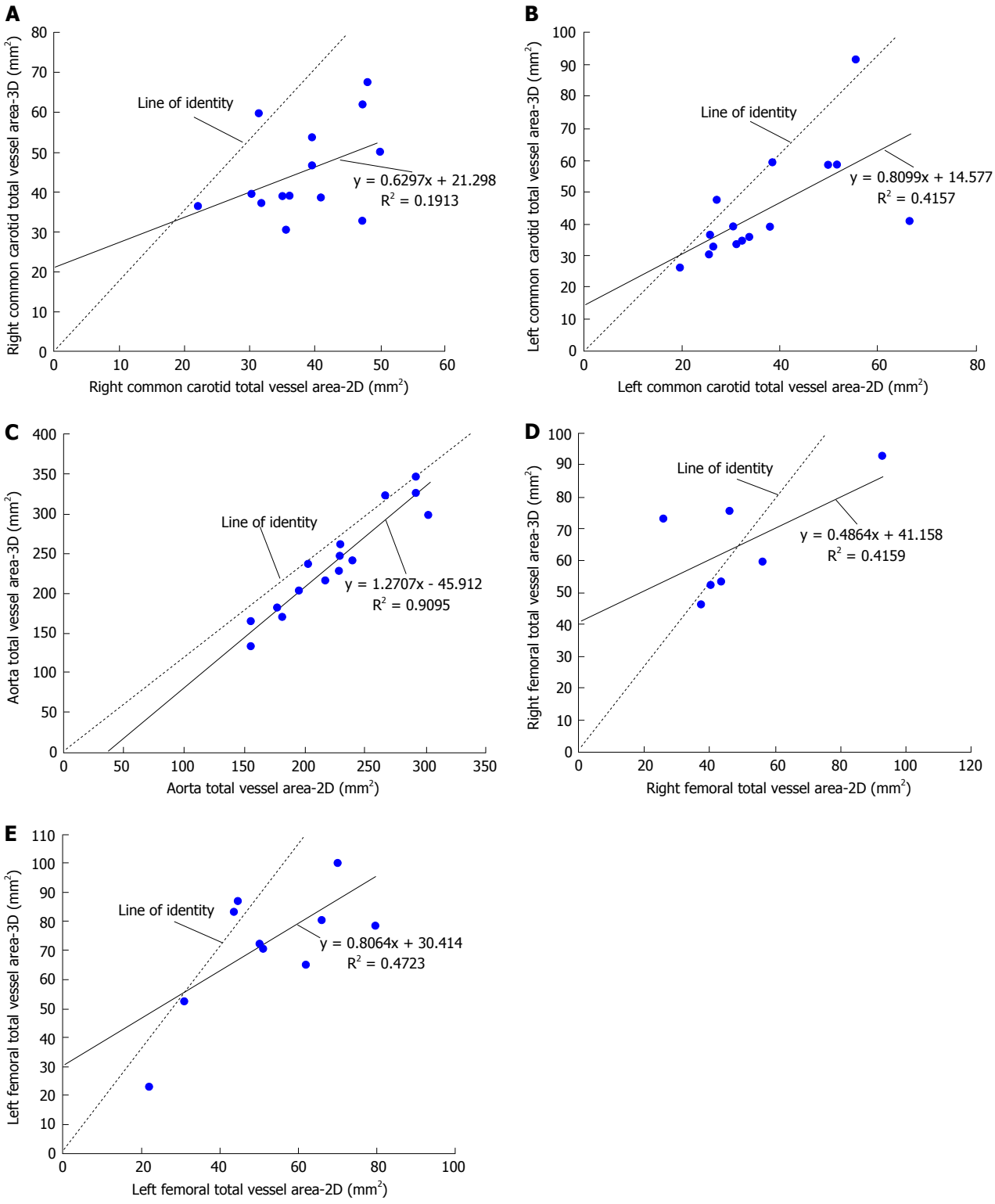

Figure 3 Scatter plots of total vessel area comparing three-dimensional SPACE and two-dimensional turbo spin echo images. A morphometric analysis using a FDA-approved, customized software program (QPlaque MR, Medis medical imaging systems, The Netherlands) was performed on all carotid, aortic and femoral arterial wall images of 16 patients who were at risk for cardiovascular or atherosclerotic disease for three-dimensional (3D) SPACE and conventional 2D multi contrast turbo spin echo (TSE) sequences. A: Scatter plot of right common carotid (RCC) total vessel area comparing 3D SPACE and 2D TSE images. There was a moderate positive linear correlation (R = 0.437) between the values of the RCC total vessel area obtained from the 3D SPACE and 2D TSE sequences; B: Scatter plot of left common carotid (LCC) total vessel area comparing 3D SPACE and 2D TSE images. There was a moderate positive linear correlation (R = 0.645) between the values of the LCC total vessel area obtained from the 3D SPACE and 2D TSE sequences; C: Scatter plot of aorta total vessel area comparing 3D SPACE and 2D TSE images. There was a strong positive linear correlation (R = 0.954) between the values of the aorta total vessel area obtained from the 3D SPACE and 2D TSE sequences; D: Scatter plot of right femoral (RF) total vessel area comparing 3D SPACE and 2D TSE images. There was a moderate positive linear correlation (R = 0.645) between the values of the RF total vessel area obtained from the 3D SPACE and 2D TSE sequences; E: Scatter plot of left femoral (LF) total vessel area comparing 3D SPACE and 2D TSE images. There was a moderate positive linear correlation (R = 0.687) between the values of the LF total vessel area obtained from the 3D SPACE and 2D TSE sequences.

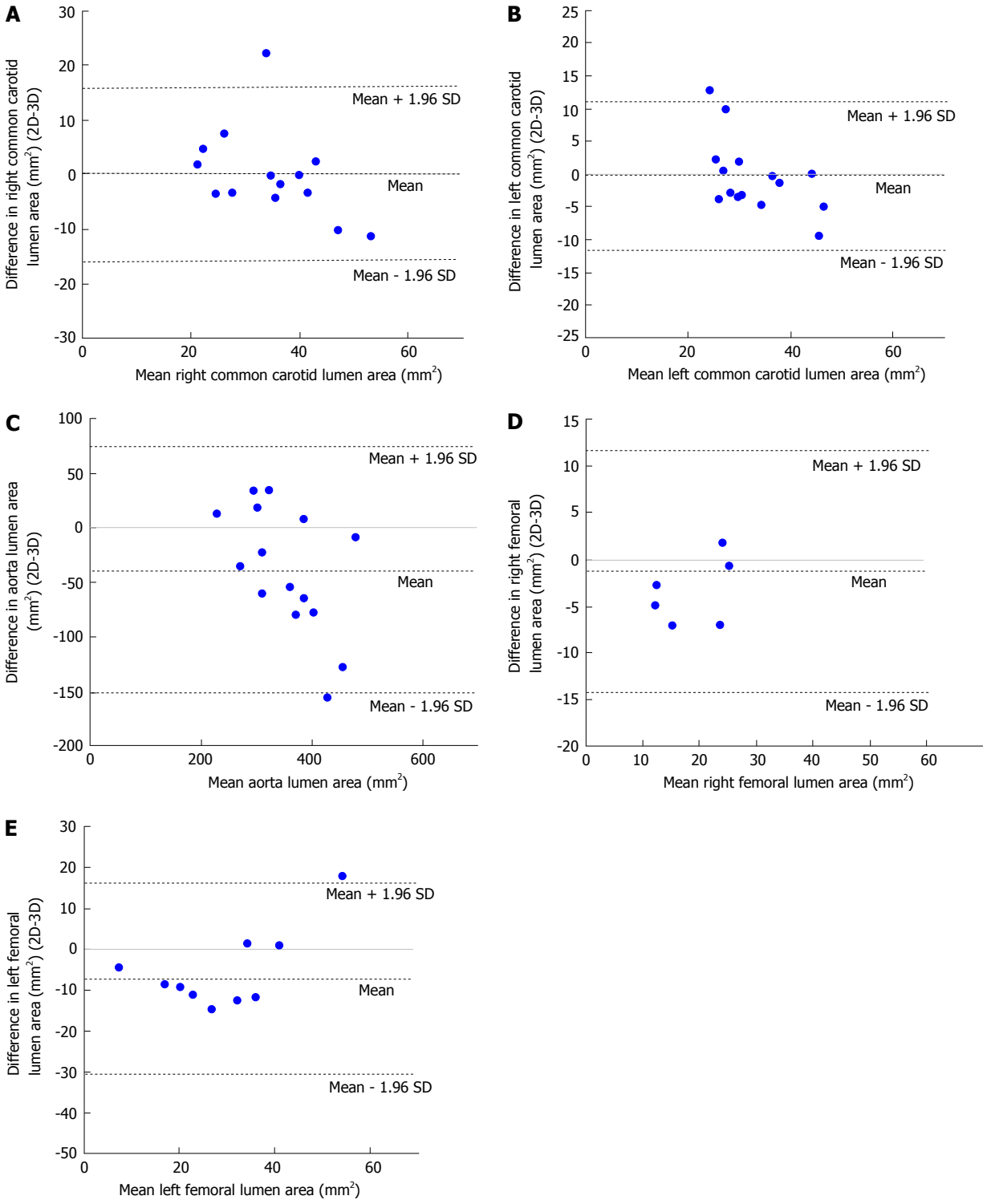

Figure 4 Bland-Altman plot of differences in lumen area (two-dimensional-three-dimensional) *vs* means of lumen area. A: Bland-Altman plot of difference in right common carotid (RCC) lumen area [two-dimensional (2D)-3D] *vs* mean RCC lumen area. Bland-Altman plot showing that the mean of the difference in RCC lumen area between 2D and 3D techniques falls on the zero line indicating that there is no bias and that the two methods are producing the same results; B: Bland–Altman plot of difference in left common carotid (LCC) lumen area (2D-3D) *vs* mean LCC lumen area. Bland-Altman plot showing that the mean of the difference in LCC lumen area between 2D and 3D techniques falls close to the zero line indicating that there is no bias and that in general the two methods are producing the same results; C: Bland-Altman plot of difference in aorta lumen area (2D-3D) *vs* mean aorta lumen area. Bland-Altman plot showing that the mean of the difference in aorta lumen area between 2D and 3D techniques falls below the zero line indicating that there is a bias and that the two methods are not producing the same results; D: Bland-Altman plot of difference in right femoral (RF) lumen area (2D-3D) *vs* mean RF lumen area. Bland-Altman plot showing that the mean of the difference in RF lumen area between 2D and 3D techniques falls below the zero line indicating that there is a bias and that the two methods are not producing the same results; E: Bland-Altman plot of difference in left femoral (LF) lumen area (2D-3D) *vs* mean LF lumen area. Bland-Altman plot showing that the mean of the difference in LF lumen area between 2D and 3D techniques falls below the zero line indicating that there is a bias and that the two methods are not producing the same results.

($P = 0.058$ and $P = 0.621$ respectively). Scatter plots of RF LA and RF TVA are shown in Figure 2D and Figure

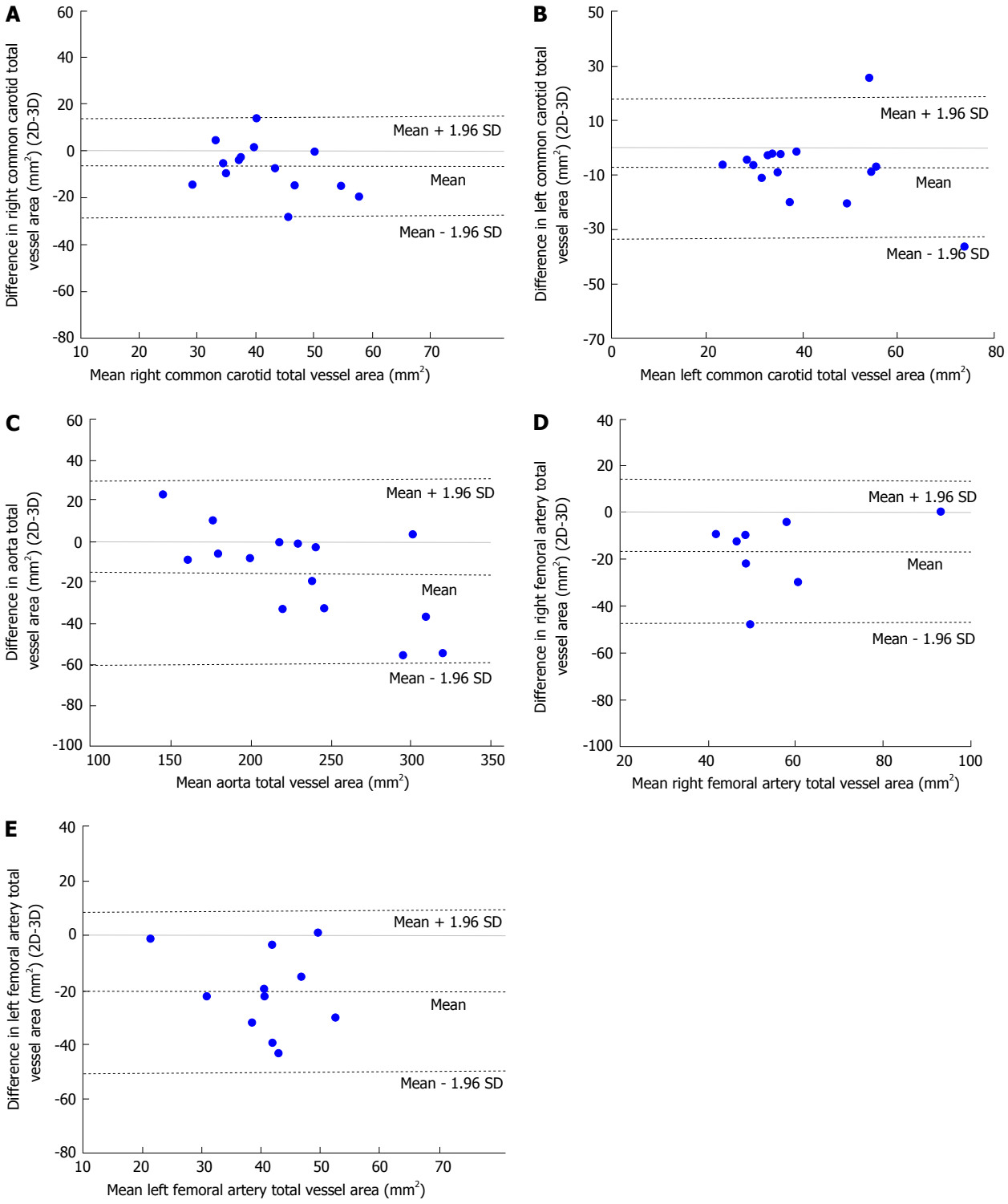

Figure 5 Bland-Altman plot of differences in total vessel area (two-dimensional-three-dimensional) *vs* means of total vessel area. A: Bland-Altman plot of difference in right common carotid (RCC) total vessel area [two-dimensional (2D)-3D] *vs* mean RCC total vessel area. Bland-Altman plot showing that the mean of the difference in RCC total vessel area between 2D and 3D techniques falls below the zero line indicating that there is a bias and that the two methods are not producing the same results; B: Bland-Altman plot of difference in left common carotid (LCC) total vessel area (2D-3D) versus mean LCC total vessel area. Bland-Altman plot showing that the mean of the difference in LCC total vessel area between 2D and 3D techniques falls below the zero line indicating that there is a bias and that the two methods are not producing the same results; C: Bland-Altman plot of difference in aorta total vessel area (2D-3D) *vs* mean aorta total vessel area. Bland-Altman plot showing that the mean of the difference in aorta total vessel area between 2D and 3D techniques falls below the zero line indicating that there is a bias and that the two methods are not producing the same results; D: Bland-Altman plot of difference in right femoral (RF) total vessel area (2D-3D) *vs* mean RF total vessel area. Bland-Altman plot showing that the mean of the difference in RF total vessel area between 2D and 3D techniques falls below the zero line indicating that there is a bias and that the two methods are not producing the same results; E: Bland-Altman plot of difference in left femoral (LF) total vessel area (2D-3D) *vs* mean LF total vessel area. Bland-Altman plot showing that the mean of the difference in LF total vessel area between 2D and 3D techniques falls below the zero line indicating that there is a bias and that the two methods are not producing the same results.

3D respectively, while that of the other aortic morphometric parameters measured are presented in the supplementary material (appendix). Bland-Altman plots of RF LA and RF TVA are shown in Figure 4D and Figure 5D respectively, while that the other aortic morphometric parameters measured are presented in the appendix. For arterial images of the LF artery, there was good correlation in all morphometric measurements from both 3D SPACE and 2D TSE sequences. The paired *t*-test results for LF images showed that significant differences were found between 3D SPACE and 2D TSE techniques in OWA, TVA, and WT, while no significant mean difference was observed between the two approaches in LA_{LF} (P = 0.066). Scatter plots of LF LA and LF TVA are shown in Figure 2E and Figure 3E respectively, while that of the other aortic morphometric parameters measured are presented in the supplementary material (appendix). Bland-Altman plots of LF LA and LF TVA are shown in Figure 4E and Figure 5E respectively, while that the other aortic morphometric parameters measured are presented in the supplementary material (appendix).

DISCUSSION

In this study carotids, aortic, and femoral arterial wall images obtained using a 3D SPACE sequence and conventional 2D TSE sequence were analyzed and compared both qualitatively and quantitatively.

Results from the qualitative assessment of carotids and aortic images using a 5-point scale showed no significant difference between the 3D and 2D approaches. However, qualitative evaluation of femoral arterial images indicated that 3D SPACE sequence fared more poorly. Scores of overall ImQ, VWD, FS, and artifacts for femoral arterial wall images from 3D SPACE sequence were significantly lower than those of images from the 2D TSE sequence. This suggests that, in comparison to the traditional 2D imaging technique, the current protocols for the 3D SPACE sequence for femoral imaging needs improvement. One potential reason for this discrepancy could also be due to the lack of a dedicated femoral imaging coil. The observed qualitative result of femoral images between the two sequences may be due to the smaller size of the femoral arteries and poorer resolution in plane of the 3D SPACE sequence or lack of specialized coils for femoral imaging. Measures addressing these aspects of the femoral imaging protocol might lead to more successful imaging outcomes of the femoral arteries in the future.

Results from the morphometric analysis showed that with respect to LA measurements for both the right and left carotids, there was no significant mean difference between the 3D SPACE and 2D TSE techniques (RCC: P = 0.941; LCC: P = 0.760). Bland-Altman plots (Figure 4A and 4B) showed no significant bias between the two imaging methodologies, and good correlation was observed between the two sequences for RCC and LCC LA measurements (Table 3). However, with respect to TVA measurements, the mean value of the 3D SPACE images for both the right and left carotids were significantly higher than the mean value of the corresponding 2D TSE images. A possible reason for the higher measurements from the 3D sequence images might be the poorer in-plane resolution of the SPACE technique (0.8 mm^2 as compared to 0.5 mm^2 of 2D in-plane resolution for carotids). When the in-plane resolution is low, the edge of the arterial wall in the image will likely be blurry which could bias the observer toward tracing a larger contour around the vessel on the image. This, in turn, would produce a higher measurement value. It could also be possible that higher area measurements from 3D SPACES images were due to the reformatting of 3D data into axial images with a slick thickness of 3.0 mm and slice gap of 1.5 mm slices comparable to those acquired by the 2D scan. However, it is fair to speculate that volume measures using 3D SPACE approach will be more robust than those from the 2D approach.

With respect to the left common carotid, aorta, and LF, our results revealed significant correlation between the 3D SPACE and 2D TSE techniques in all morphometric measurements including outer wall area, LA, total wall area, and WT. With respect to the RF, good correlation between the two sequences was noted for LA and vessel wall area. Overall, our quantitative results indicated that morphometric parameter measurements obtained from 3D SPACE images demonstrated good agreement with those from 2D TSE technique.

Results of the current study demonstrated that LA measurements with respect to the left and right common carotids from the 3D SPACE technique are comparable to those of 2D TSE technique. This suggests that 3D SPACE might be a feasible imaging approach for determining overall plaque burden in the bilateral carotids.

Despite significant mean differences in TVA across all three vascular beds, good agreement was observed between the two sequences indicating that with respect to TVA, 3D SPACE technique might still be feasibly comparable to the 2D TSE technique.

Using the current approach, 3D SPACE is suboptimal for femoral imaging. However, this may be due to coils not being optimized for femoral imaging. Given that 3D SPACE technique may provide more accurate volumetric burden measurements due to decreased susceptibility to volume averaging artifacts and improved vessel wall coverage, further research is warranted to establish stronger evidence for the optimum reproducibility of imaging results of the 3D SPACE technique.

Limitations

It is a limitation that a number of our quantitative assessments-including analyses of the femoral arteries, involved a small number of patients. The small number of patients presented problems in the interpretation of results. Further assessment comparing imaging results obtained using both 3D SPACE and conventional 2D TSE sequences in evaluating the three different vascular beds in

a larger cohort of patients is warranted. In addition, coils used were not optimized for femoral imaging. This may have affected the results.

ACKNOWLEDGMENTS

The authors wish to thank Dr. Claudia Calcagno for help with scanning and Tayo Davies for help with patient recruitment.

COMMENTS

Background

Atherosclerosis, a systemic disease affecting all vascular beds, leads to cardiovascular morbidity and mortality. In the evaluation of atherosclerosis and blood vessel wall morphology, magnetic resonance imaging (MRI) has emerged as the leading non-invasive *in vivo* imaging modality. Three-dimensional (3D) black blood MRI technique is now being used to evaluate progression of atherosclerosis over time and changes in response to therapy. A 3D black blood turbo spin echo (TSE) sequence approach of interest is the sampling perfection with application-optimized contrast using different flip angle evolution (SPACE). Before SPACE can become widely accepted, however, its effectiveness in assessing multiple vascular territories must first be established.

Research frontiers

In the area of atherosclerotic plaque imaging, the research hotspot is optimizing an MRI technique that will enhance MRI images and better visualize atherosclerotic plaque burden and vessel wall morphology.

Innovations and breakthroughs

3D black blood MRI is becoming the leading technique in evaluating atherosclerosis and blood vessels. Compared to conventional 2D approaches, 3D black blood has a higher SNR and decreased susceptibility of volume averaging artifacts. In addition, it has the ability to obtain isotropic voxels thereby enabling multi-planar reformatting of images. 3D techniques are used to assess systemic disease burden as a whole, instead of being concentrated on a single lesion. Furthermore, they can be used in the evaluation of multiple vascular beds including the carotids, aorta, and femoral arteries.

Applications

The study results suggest that 3D SPACE may be a feasible approach in the evaluation of cardiovascular patients.

Terminology

Black blood MRI is achieved when blood flow and lumen signals are suppressed allowing for better visualization of the vessel wall. Normally, in contrast-enhanced MRI images, the blood flow and lumen are hyper-intense and bright. In black blood imaging, the reverse happens. The lumen and blood are dark, while the vessel walls appear bright.

Peer review

This study compared the 3D SPACE *vs* 2D TSE qualitatively and quantitatively using carotid, aorta, and femoral arteries. In general, the manuscript was clearly written and investigated two sequences clearly.

REFERENCES

1 **Mani V**, Wong SK, Sawit ST, Calcagno C, Maceda C, Ramachandran S, Fayad ZA, Moline J, McLaughlin MA. Relationship between particulate matter exposure and atherogenic profile in "Ground Zero" workers as shown by dynamic contrast enhanced MR imaging. *Int J Cardiovasc Imaging* 2013; **29**: 827-833 [PMID: 23179748 DOI: 10.1007/s10554-012-0154-x]

2 **Sanz J**, Fayad ZA. Imaging of atherosclerotic cardiovascular disease. *Nature* 2008; **451**: 953-957 [PMID: 18288186 DOI: 10.1038/nature06803]

3 **El Aidi H**, Mani V, Weinshelbaum KB, Aguiar SH, Taniguchi H, Postley JE, Samber DD, Cohen EI, Stern J, van der Geest RJ, Reiber JH, Woodward M, Fuster V, Gidding SS, Fayad ZA. Cross-sectional, prospective study of MRI reproducibility in the assessment of plaque burden of the carotid arteries and aorta. *Nat Clin Pract Cardiovasc Med* 2009; **6**: 219-228 [PMID: 19174763 DOI: 10.1038/ncpcardio1444]

4 **Toussaint JF**, LaMuraglia GM, Southern JF, Fuster V, Kantor HL. Magnetic resonance images lipid, fibrous, calcified, hemorrhagic, and thrombotic components of human atherosclerosis in vivo. *Circulation* 1996; **94**: 932-938 [PMID: 8790028]

5 **Fayad ZA**, Nahar T, Fallon JT, Goldman M, Aguinaldo JG, Badimon JJ, Shinnar M, Chesebro JH, Fuster V. In vivo magnetic resonance evaluation of atherosclerotic plaques in the human thoracic aorta: a comparison with transesophageal echocardiography. *Circulation* 2000; **101**: 2503-2509 [PMID: 10831525]

6 **Yuan C**, Kerwin WS, Yarnykh VL, Cai J, Saam T, Chu B, Takaya N, Ferguson MS, Underhill H, Xu D, Liu F, Hatsukami TS. MRI of atherosclerosis in clinical trials. *NMR Biomed* 2006; **19**: 636-654 [PMID: 16986119]

7 **Mani V**, Muntner P, Gidding SS, Aguiar SH, El Aidi H, Weinshelbaum KB, Taniguchi H, van der Geest R, Reiber JH, Bansilal S, Farkouh M, Fuster V, Postley JE, Woodward M, Fayad ZA. Cardiovascular magnetic resonance parameters of atherosclerotic plaque burden improve discrimination of prior major adverse cardiovascular events. *J Cardiovasc Magn Reson* 2009; **11**: 10 [PMID: 19393089 DOI: 10.1186/1532-429X-11-10]

8 **Calcagno C**, Ramachandran S, Izquierdo-Garcia D, Mani V, Millon A, Rosenbaum D, Tawakol A, Woodward M, Bucerius J, Moshier E, Godbold J, Kallend D, Farkouh ME, Fuster V, Rudd JH, Fayad ZA. The complementary roles of dynamic contrast-enhanced MRI and 18F-fluorodeoxyglucose PET/CT for imaging of carotid atherosclerosis. *Eur J Nucl Med Mol Imaging* 2013; **40**: 1884-1893 [PMID: 23942908 DOI: 10.1007/s00259-013-2518-4]

9 **Isbell DC**, Meyer CH, Rogers WJ, Epstein FH, DiMaria JM, Harthun NL, Wang H, Kramer CM. Reproducibility and reliability of atherosclerotic plaque volume measurements in peripheral arterial disease with cardiovascular magnetic resonance. *J Cardiovasc Magn Reson* 2007; **9**: 71-76 [PMID: 17178683]

10 **Briley-Saebo KC**, Mulder WJ, Mani V, Hyafil F, Amirbekian V, Aguinaldo JG, Fisher EA, Fayad ZA. Magnetic resonance imaging of vulnerable atherosclerotic plaques: current imaging strategies and molecular imaging probes. *J Magn Reson Imaging* 2007; **26**: 460-479 [PMID: 17729343]

11 **Balu N**, Chu B, Hatsukami TS, Yuan C, Yarnykh VL. Comparison between 2D and 3D high-resolution black-blood techniques for carotid artery wall imaging in clinically significant atherosclerosis. *J Magn Reson Imaging* 2008; **27**: 918-924 [PMID: 18383253 DOI: 10.1002/jmri.21282]

12 **Keenan NG**, Grasso A, Locca D, Varghese A, Roughton M, Gatehouse PD, Firmin DN, Pennell DJ. Comparison of 2D and multislab 3D magnetic resonance techniques for measuring carotid wall volumes. *J Magn Reson Imaging* 2008; **28**: 1476-1482 [PMID: 19025935 DOI: 10.1002/jmri.21582]

13 **Mani V**, Aguiar SH, Itskovich VV, Weinshelbaum KB, Postley JE, Wasenda EJ, Aguinaldo JG, Samber DD, Fayad ZA. Carotid black blood MRI burden of atherosclerotic disease assessment correlates with ultrasound intima-media thickness. *J Cardiovasc Magn Reson* 2006; **8**: 529-534 [PMID: 16755842]

14 **Koktzoglou I**, Chung YC, Mani V, Carroll TJ, Morasch MD, Mizsei G, Simonetti OP, Fayad ZA, Li D. Multislice dark-blood carotid artery wall imaging: a 1.5 T and 3.0 T comparison. *J Magn Reson Imaging* 2006; **23**: 699-705 [PMID: 16555260]

15 **Koktzoglou I**, Li D. Diffusion-prepared segmented steady-state free precession: Application to 3D black-blood cardiovascular magnetic resonance of the thoracic aorta and carotid artery walls. *J Cardiovasc Magn Reson* 2007; **9**: 33-42 [PMID: 17178678]

16 **Hayashi K**, Mani V, Nemade A, Silvera S, Fayad ZA. Com-

parison of 3D-diffusion-prepared segmented steady-state free precession and 2D fast spin echo imaging of femoral artery atherosclerosis. *Int J Cardiovasc Imaging* 2010; **26**: 309-321 [PMID: 19946750 DOI: 10.1007/s10554-009-9544-0]

17 **Underhill HR**, Hatsukami TS, Fayad ZA, Fuster V, Yuan C. MRI of carotid atherosclerosis: clinical implications and future directions. *Nat Rev Cardiol* 2010; **7**: 165-173 [PMID: 20101259 DOI: 10.1038/nrcardio.2009.246]

18 **Zhang Z**, Fan Z, Carroll TJ, Chung Y, Weale P, Jerecic R, Li D. Three-dimensional T2-weighted MRI of the human femoral arterial vessel wall at 3.0 Tesla. *Invest Radiol* 2009; **44**: 619-626 [PMID: 19692844 DOI: 10.1097/RLI.0b013e3181b4c218]

19 **Yarnykh VL**, Terashima M, Hayes CE, Shimakawa A, Takaya N, Nguyen PK, Brittain JH, McConnell MV, Yuan C. Multicontrast black-blood MRI of carotid arteries: comparison between 1.5 and 3 tesla magnetic field strengths. *J Magn Reson Imaging* 2006; **23**: 691-698 [PMID: 16555259]

20 **Itskovich VV**, Mani V, Mizsei G, Aguinaldo JG, Samber DD, Macaluso F, Wisdom P, Fayad ZA. Parallel and nonparallel simultaneous multislice black-blood double inversion recovery techniques for vessel wall imaging. *J Magn Reson Imaging* 2004; **19**: 459-467 [PMID: 15065170]

21 **Itskovich VV**, Samber DD, Mani V, Aguinaldo JG, Fallon JT, Tang CY, Fuster V, Fayad ZA. Quantification of human atherosclerotic plaques using spatially enhanced cluster analysis of multicontrast-weighted magnetic resonance images. *Magn Reson Med* 2004; **52**: 515-523 [PMID: 15334569]

22 **Mani V**, Itskovich VV, Aguiar SH, Mizsei G, Aguinaldo JG, Samber DD, Macaluso FM, Fayad ZA. Comparison of gated and non-gated fast multislice black-blood carotid imaging using rapid extended coverage and inflow/outflow saturation techniques. *J Magn Reson Imaging* 2005; **22**: 628-633 [PMID: 16215965]

23 **Mani V**, Itskovich VV, Szimtenings M, Aguinaldo JG, Samber DD, Mizsei G, Fayad ZA. Rapid extended coverage simultaneous multisection black-blood vessel wall MR imaging. *Radiology* 2004; **232**: 281-288 [PMID: 15220509]

24 **Fayad ZA**, Mani V, Woodward M, Kallend D, Abt M, Burgess T, Fuster V, Ballantyne CM, Stein EA, Tardif JC, Rudd JH, Farkouh ME, Tawakol A. Safety and efficacy of dalcetrapib on atherosclerotic disease using novel non-invasive multimodality imaging (dal-PLAQUE): a randomised clinical trial. *Lancet* 2011; **378**: 1547-1559 [PMID: 21908036 DOI: 10.1016/S0140-6736(11)61383-4]

25 **Fayad ZA**, Mani V, Woodward M, Kallend D, Bansilal S, Pozza J, Burgess T, Fuster V, Rudd JH, Tawakol A, Farkouh ME. Rationale and design of dal-PLAQUE: a study assessing efficacy and safety of dalcetrapib on progression or regression of atherosclerosis using magnetic resonance imaging and 18F-fluorodeoxyglucose positron emission tomography/computed tomography. *Am Heart J* 2011; **162**: 214-221.e2 [PMID: 21835280 DOI: 10.1016/j.ahj.2011.05.006]

26 **Hayashi K**, Mani V, Nemade A, Aguiar S, Postley JE, Fuster V, Fayad ZA. Variations in atherosclerosis and remodeling patterns in aorta and carotids. *J Cardiovasc Magn Reson* 2010; **12**: 10 [PMID: 20205722 DOI: 10.1186/1532-429X-12-10]

P- Reviewers: Beeres M, Shin C **S- Editor**: Ji FF
L- Editor: A **E- Editor**: Liu SQ

Published by **Baishideng Publishing Group Inc**
8226 Regency Drive, Pleasanton, CA 94588, USA
Telephone: +1-925-223-8242
Fax: +1-925-223-8243
E-mail: bpgoffice@wjgnet.com
Help Desk: http://www.wjgnet.com/esps/helpdesk.aspx
http://www.wjgnet.com